ARTICLE

Superhydrophobic and Self-Cleaning Bio-Fiber Surfaces via ATRP and Subsequent Postfunctionalization

Daniel Nyström, Josefina Lindqvist, Emma Östmark, Per Antoni, Anna Carlmark, Anders Hult, and Eva Malmström*

Department of Fibre and Polymer Technology, KTH School of Chemical Science and Engineering, Royal Institute of Technology, Teknikringen 56-58, Stockholm, Sweden

ABSTRACT Superhydrophobic and self-cleaning cellulose surfaces have been obtained via surface-confined grafting of glycidyl methacrylate using atom transfer radical polymerization combined with postmodification reactions. Both linear and branched graft-on-graft architectures were used for the postmodification reactions to obtain highly hydrophobic bio-fiber surfaces by functionalization of the grafts with either poly(dimethylsiloxane), perfluorinated chains, or alkyl chains, respectively. Postfunctionalization using alkyl chains yielded results similar to those of surfaces modified by perfluorination, in terms of superhydrophobicity, self-cleaning properties, and the stability of these properties over time. In addition, highly oleophobic surfaces have been obtained when modification with perfluorinated chains was performed.

KEYWORDS: superhydrophobic • self-cleaning • cellulose surface • ATRP • alkyl chain • perfluorinated alkyl chain • poly(dimethylsiloxane)

INTRODUCTION

The remarkable properties of superhydrophobic surfaces, including self-cleaning ability and water repellency, have attracted much academic and industrial interest recently because of the potential use of such surfaces in various applications (1, 2). Inspired by Mother Nature's examples of these types of surfaces, present in plant leaves such as the Lotus leaf and insects such as the water strider (3, 4), researchers have utilized a great variety of techniques to obtain the same properties synthetically (5−19). Truly superhydrophobic surfaces, with a water contact angle (CA) above 150° and low CA hysteresis, require a certain surface roughness because chemical composition alone is insufficient to create superhydrophobicity (17−23). The superhydrophobicity and self-cleaning properties of the Lotus leaf is obtained via a combination of low-energy compounds and a binary structure of micro- and nanometer textures (3).

The need for renewable materials with improved material properties is steadily increasing, and the desire to modify bio-based materials, such as cellulose, for new application areas has emerged during recent years. For example, the fabrication of superhydrophobic cellulose surfaces could extend the use of cellulose and its derivatives into new areas such as self-cleaning textiles, water repellent packaging materials, and coatings with improved barrier properties.

Cellulose is an abundant, inexpensive, biodegradable, and renewable biopolymer exhibiting excellent mechanical properties (24, 25). However, the use of cellulose in more advanced applications typically requires modification to alter and/or tailor its chemical and physical properties (24, 25). Our group has focused on surface modification of bio-based substrates by atom transfer radical polymerization (ATRP) using the "grafting-from" methodology, where the polymer brushes are formed in situ from surface-confined initiating sites (26−33). For example, nanosized containers based on cellulose (31), dual-responsive cellulose surfaces (32), and cellulose surfaces with liquid-crystalline surface properties (33) have been synthesized.

ATRP is a controlled radical polymerization technique that has been proven useful for the synthesis of functional macromolecules with controlled and complex architectures (34−38). Surface-initiated ATRP has also been used for the modification of a variety of other substrates (39−48). The great advantage of ATRP compared to free-radical polymerization is the ability to control the length of the grafted polymer chains and thereby tailor the properties of the modified surface. Also, the dormant halide−carbon bond present at the chain ends can be reactivated and is therefore available for further (polymerization) reactions.

In order to convert hydrophilic cellulose into a highly hydrophobic material, the incorporation of low surface energy compounds is necessary. There are reports in the literature describing the fabrication of superhydrophobic (cotton/cellulose) textiles (49−54). Different approaches, such as reduction of gold particles onto texiles (49), decoration of textiles with nanoparticles combined with a monolayer of polymer (51), and attachment of a silicone coating, have been utilized to obtain superhydrophobic textiles (52).

* To whom correspondence should be addressed. E-mail: mavem@kth.se. Fax: +46 8790 8283. Tel: +46 8790 8273.
Received for review December 12, 2008 and accepted February 18, 2009

DOI: 10.1021/am800235e

Published on Web 03/24/2009

We have previously reported a method based on the combination of ATRP of glycidyl methacrylate (GMA) and postfunctionalization using a perfluorinated acid chloride in order to create superhydrophobic and self-cleaning bio-based materials (29). Herein, we present our continued work regarding the fabrication of superhydrophobic bio-based fiber surfaces using ATRP of GMA and subsequent functionalization techniques. Because of environmental concerns caused by fluorine-containing compounds and their high cost, we have investigated the possibility of obtaining superhydrophobic, highly oleophobic, and self-cleaning cellulose surfaces using reduced amounts of fluorine or even by complete replacement of fluorine with other hydrophobic compounds such as long alkyl chains or poly(dimethylsiloxane) (PDMS). The main question addressed in the present study is to what extent the functionalized cellulose surfaces maintain their hydrophobic character over time.

EXPERIMENTAL SECTION

Materials. Copper(I) chloride ($Cu^{I}Cl$; 99+%), copper(II) bromide ($Cu^{II}Br_2$; 99%), *N*,*N*,*N*′,*N*″,*N*″-pentamethyldiethylenetriamine (PMDETA; 99%), 2-bromisobutyryl bromide (98%), pentadecafluorooctanoyl chloride (97%), heptafluorobutyryl chloride (98%), palmitoyl chloride (98%), bis(3-aminopropyl)-terminated poly(dimethylsiloxane) (PDMS; average $M_w = 2500$), and Whatman 1 filter paper were used as received from Aldrich. 4-(Dimethylamino)pyridine (DMAP; 99%), concentrated hydrochloric acid (HCl), and triethylamine (TEA; 99%) were used as received from Acros. Glycidyl methacrylate (GMA; 97 %) was also acquired from Acros but passed through a column of neutral aluminum oxide prior to use.

Instrumentation. Infrared spectra were recorded on a Perkin-Elmer Spectrum 2000 Fourier transform infrared (FT-IR) spectrometer equipped with a MKII Golden Gate, single reflection ATR System from Specac Ltd., London, U.K. The ATR crystal was a MKII heated Diamond 45° ATR top plate. The bio-fiber surface was pressed against the ATR crystal to obtain a sufficient signal.

CA measurements were performed at 50% relative humidity and 23 °C and conducted on a KSV Instruments CAM 200 equipped with a Basler A602f camera, using 5 μL droplets of Milli-Q water. The water CAs were determined using the CAM software.

Imaging of the surfaces was performed in tapping mode on a NanoScope IIIa Multimode atomic force microscopy (AFM) instrument, using silicon tips (supplied by Veeco) with resonance frequencies of 267−348 kHz (according to the manufacturer).

Immobilization of 2-Bromoisobutyryl Bromide on Filter Paper. The procedure for attachment of the initiator to the surface was adopted from Carlmark and Malmström (26). Prior to immobilization of the initiator, the filter paper (2 × 3 cm) was washed with acetone and tetrahydrofuran (THF) and subsequently ultrasonicated in both solvents. The accessible hydroxyl groups on the cellulose surface were then converted into ATRP initiators by immersing the cellulose surface in a solution containing 2-bromoisobuturyl bromide (305 mg, 1.33 mmol), TEA (148 mg, 1.46 mmol), and a catalytic amount of DMAP in THF (20 mL). The reaction was allowed to proceed overnight at room temperature on a shaking device. After the reaction was completed, the filter paper was thoroughly washed with EtOH and THF successively to remove residual reactants and byproducts. The filter paper was finally dried under vacuum at 50 °C overnight. This procedure was also employed for the immobilization of 2-bromoisobutyryl bromide onto hydrolyzed PGMA-modified bio-fiber surfaces.

Grafting of GMA from 2-Bromoisobutyrate-Functionalized Filter Paper. The initiator-modified filter paper was immersed in a flask containing toluene (4 mL), GMA (4.30 g, 30.2 mmol), $Cu^{I}Cl$ (14.0 mg, 141 μmol), $Cu^{II}Br_2$ (4.0 mg, 17 μmol), and PMDETA (25.0 mg, 140 μmol). The flask was sealed with a rubber septum and thereafter evacuated and back-filled with argon three times. Grafting of GMA from the initiator-modified filter paper was conducted at 30 °C and allowed to proceed for 40−120 min. After the polymerization was completed, the filter paper was thoroughly washed with THF, dichloromethane (DCM), MeOH, THF/H_2O, and MeOH successively to remove residual monomer and the catalyst. The filter paper was finally dried under vacuum at 50 °C overnight. This procedure was also employed in the fabrication of graft-on-graft PGMA-modified bio-fiber surfaces.

Hydrolysis of the Epoxide Group. The epoxide groups in the PGMA-grafted filter paper were hydrolyzed in a solution of THF (10 mL), 12 drops of H_2O, and 12 drops of concentrated HCl. The reaction was allowed to proceed for 60 min; the substrate was thereafter rinsed with THF, H_2O, EtOH, and MeOH successively and finally dried under vacuum at 50 °C overnight.

Attachment of Pentadecafluorooctanoyl Chloride (C_7F_{15}) to Hydrolyzed PGMA-Grafted Filter Paper. The hydrolyzed PGMA-grafted filter paper was immersed in a round-bottomed flask containing DCM (10 mL), TEA (74.0 mg, 730 μmol), and DMAP (catalytic amount). C_7F_{15} (288 mg, 670 μmol) was added dropwise, and the acylation reaction was allowed to proceed overnight. After the reaction was completed, the filter paper was rinsed with THF, DCM, EtOH, and THF successively. The filter paper was finally dried under vacuum at 50 °C overnight. The other acylation reactions were performed in a similar manner using the same molar amounts of acid chlorides as those in the example above.

Attachment of Bis(3-aminopropyl)-Terminated PDMS to PGMA-Grafted Filter Paper. The PGMA-grafted filter paper was immersed in a round-bottomed flask containing toluene (6 mL) and amine-functional PDMS (500.0 mg, 0.2 mmol). The reaction was allowed to proceed at 100 °C overnight; the filter paper was thereafter rinsed with toluene, THF, DCM, and MeOH and finally dried under vacuum at 50 °C.

RESULTS AND DISCUSSION

We have previously reported on the fabrication of superhydrophobic and self-cleaning bio-fiber surfaces using surface-initiated ATRP of GMA combined with postfunctionalization using C_7F_{15} (29).

Fluorine-containing compounds suffer, however, from some disadvantages including the economic and environmental aspects; the compounds are costly and are also known to have a negative impact on the environment and human health. In this study, we have therefore investigated the possibility of accomplishing superhydrophobic surfaces using reduced amounts of fluorine and also the complete replacement of fluorine groups by other hydrophobic and more environmentally friendly compounds such as long alkyl chains or PDMS.

A series of hydrophobic surfaces were prepared and carefully characterized (FT-IR, AFM, CA, CA over time, CA hysteresis, oleophobic properties, and self-cleaning ability).

Surface Modification of Bio-fiber Substrates To Obtain Superhydrophobic Surfaces. Filter paper was chosen as the bio-fiber substrate because of its high inherent surface roughness, which will facilitate an increased hydrophobic character (17−22). Also, the use of filter paper

Scheme 1. Synthetic Approach to Functionalization of Bio-Fiber Surfaces[a]

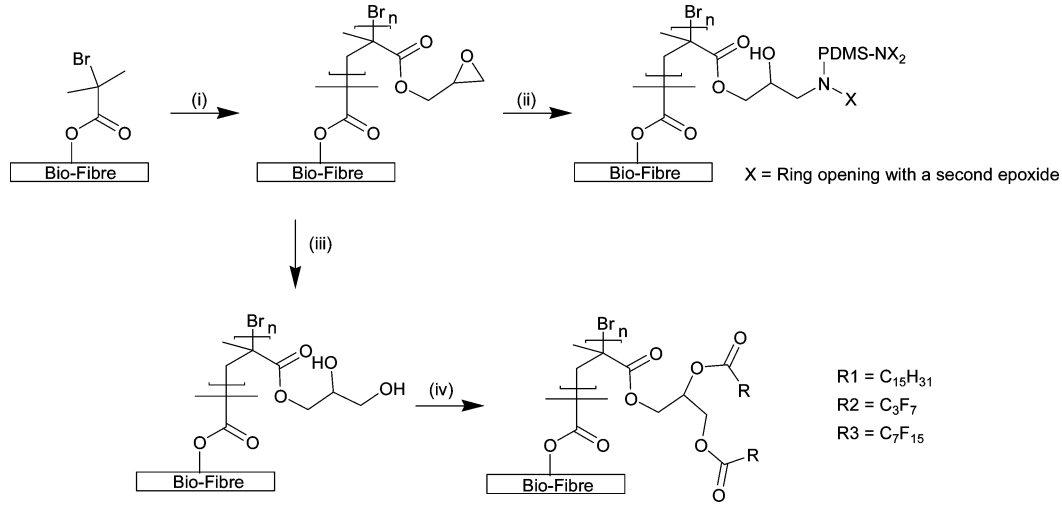

[a] Conditions: (i) GMA, $Cu^{I}Cl$, $Cu^{II}Br_2$, PMDETA, toluene, 30 °C; (ii) toluene, bis(3-aminopropyl)-terminated PDMS, 100 °C; (iii) HCl(aq), THF, RT; (iv) acid chloride (R1−R3), TEA, DMAP, DCM, RT.

will generate a flexible surface that can be folded without disruption of the hydrophobic nature.

We have previously shown that the direct acylation of the hydroxyl groups on the cellulose surface using C_7F_{15} did not result in sufficient surface coverage to yield a superhydrophobic surface over a prolonged period of time (29). In order to increase the surface coverage and thereby also the thickness of the hydrophobic layer on the cellulose surface, GMA was grafted from the cellulose surface via surface-initiated ATRP. PGMA is an interesting polymer because its epoxide groups can be considered as protected 1,2-diols and it can subsequently be used as a reactive handle for postfunctionalization reactions (55−59). Grafting of GMA from the filter paper was conducted at 30 °C in toluene and was catalyzed by $Cu^{I}Cl$, $Cu^{II}Br_2$, and PMDETA, as previously described (Scheme 1) (29). The residual monomer and the catalyst complex were removed from the bio-fiber surface by extensive washing in different solvents. The success of the grafting of PGMA from the filter paper was confirmed by FT-IR analysis, showing the carbonyl stretch at 1730 cm^{-1}. The carbonyl stretch increased with increasing polymerization time, thus indicating a controlled polymerization (see the Supporting Information).

Postfunctionalization of the PGMA-modified cellulose substrates was performed with four different compounds: C_7F_{15}, heptafluorobutyryl chloride (C_3F_7), palmitoyl chloride, and PDMS. The longer fluoroalkyl chain (C_7F_{15}) was used in our previous work, and in the present study, we wanted to compare this compound with more attractive ones. The shorter fluoroalkyl chain (C_3F_7) was chosen as an alternative compound to C_7F_{15}, because it contains less fluorine but is still a known hydrophobic compound. Palmitoyl chloride, containing a long alkyl chain ($C_{15}H_{31}$) and bis(3-aminopropyl)-terminated PDMS, is also known to be hydrophobic and was used to investigate whether it was possible to obtain highly hydrophobic surfaces completely without fluorine.

To achieve functionalization using C_7F_{15}, C_3F_7, and palmitoyl chloride, the pendant epoxide groups in the PGMA grafts were hydrolyzed under acidic conditions using HCl in THF to generate hydroxyl-functional polymer grafts (Scheme 1). The hydrolysis was confirmed via FT-IR spectroscopy, where a broadening of the carbonyl stretch was observed, and also by an increased wettability (hydrophilicity) of the surface. The postfunctionalization reactions were confirmed with FT-IR via the appearance of a carbonyl stretch at 1800 cm^{-1} for the fluorinated surfaces and at 1730 cm^{-1} for the surface postfunctionalized with palmitoyl chloride (see the Supporting Information).

For postfunctionalization using PDMS, the reaction was performed directly with the epoxide groups on the PGMA grafts (Scheme 1). It is proposed that each amine reacts ultimately with two epoxide groups, suggesting the formation of a cross-linked network. The reaction was confirmed via FT-IR by the appearance of the siloxane groups at 805 cm^{-1} (see the Supporting Information).

Characterization of Postfunctionalized PGMA-Grafted Surfaces. The cellulose surfaces modified with linear PGMA grafts were postfunctionalized in four different ways as described above, and the hydrophobicity of the resulting surfaces was assessed with water CA measurements. It should be noted that the CA is somewhat difficult to measure on filter paper, because of the fibrillar structure of the cellulose, rendering it problematic to set the baseline for the surface and water droplet. It is well-known that surfaces with high CAs can be obtained by combining low-energy compounds with high surface roughness. However, one important parameter, often not reported when dealing with superhydrophobic surfaces, is the CA hysteresis. The hysteresis, calculated as the difference between the advancing CA and the receding CA, is of utmost importance for the movement of water droplets on the surface (17−22). A low hysteresis renders the surface "nonsticky", a property that is crucial for the fabrication of water-repellent and self-cleaning surfaces. The static, advancing, and receding CAs

Table 1. CA Results Obtained for PGMA Graft Architectures Modified with Different Low-Energy Compounds

	CA (deg)			
single graft	static	advancing	receding	hysteresis
PGMA−C_7F_{15}	161	168	159	9
PGMA−C_3F_7	157	161	155	6
PGMA−$C_{15}H_{31}$	159	162	155	7
PGMA−PDMS	155	161	150	11

for the postfunctionalized PGMA-grafted cellulose surfaces are displayed in Table 1.

The highest CA, 161°, was obtained for the surface postfunctionalized with the longer fluoroalkyl chain (C_7F_{15}; Figure 1 and Table 1). A low hysteresis of 9° was also observed for this surface. Postfunctionalization with the shorter fluoroalkyl chain (C_3F_7) still yielded a high static CA (157°) and an even lower hysteresis than was obtained using the longer flouroalkyl chain (C_3F_7; Figure 1 and Table 1). Interestingly, this demonstrated that the hydrophobic nature is maintained even though a perfluorinated acid chloride with fewer fluorine groups is used. For the surface postfunctionalized with the long alkyl chain, the obtained CA was around 159° and the hysteresis 7°, similar values to those obtained for the fluorinated surfaces, indicating that a superhydrophobic surface was obtained without the use of fluorine ($C_{15}H_{31}$; Figure 1 and Table 1). In addition, the PDMS-modified bio-fiber surface was found to be superhydrophobic with a CA of 155° (PDMS; Figure 1 and Table 1). The static CA for the PDMS surface is in agreement with the result that Ming and co-workers obtained for cotton textiles modified with silica particles in combination with PDMS (50). The hysteresis of 11° is, however, higher than those for the other surfaces studied in the series.

Even though all of the surfaces based on linear PGMA graft copolymerization were found to be superhydrophobic from CA measurements, they did not retain this superhydrophobicity over prolonged periods of time. The stability of the CA over time is a very important parameter for superhydrophobic surfaces, providing information about the long-time surface dynamics. Unfortunately, results from long-time stability measurements are seldom reported. We found that the CA decreased from 161° to 138° over 1 h for the C_7F_{15}-modified PGMA-grafted surface. A similar drop was observed for the C_3F_7-modified surface, and the CA for the surface functionalized with $C_{15}H_{31}$ decreased even more, exhibiting 127° after 1 h.

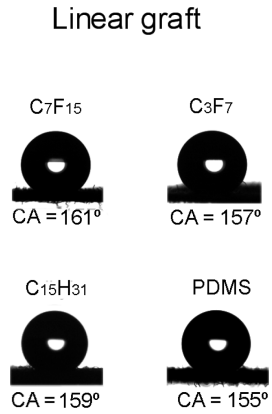

FIGURE 1. CA images for PGMA graft architectures modified with different low-energy compounds (Table 1).

Fabrication of Superhydrophobic Surfaces via Postfunctionalization of a Branched Graft-on-Graft Architecture. Conclusively, the bio-fiber surfaces obtained via postfunctionalization of PGMA brushes with different low-energy compounds were superhydrophobic and had a low hysteresis. The surfaces did not, however, exhibit permanent superhydrophobicity over an extended time period (1 h). In order to create a surface capable of maintaining its superhydrophobic character, a new route had to be explored. The route was based on immobilization of 2-bromoisobutyryl bromide onto the hydroxyl groups of the hydrolyzed epoxide groups in the PGMA-grafted bio-fiber surface, resulting in a multitude of initiators along the backbone of each chain (29). A branched graft-on-graft architecture was obtained when PGMA was grafted from each brush (Scheme 2).

Characterization of Postfunctionalized PGMA-*g*-PGMA Surfaces. *Hydrophobicity.* The postfunctionalized PGMA-modified graft-on-graft surfaces were characterized by CA measurements. The static, advancing, and receding CAs can be found in Table 2.

The attachment of C_7F_{15} to the graft-on-graft modified surfaces resulted in the highest hydrophobicity. These surfaces showed a significant increase in hydrophobicity compared to the linear graft modification, and an extremely high CA of 172° and a very low hysteresis of 5° were obtained (C_7F_{15}; Figure 2 and Table 2). The postfunctionalization using C_3F_7 rendered a small increase in CA as compared to the functionalization of the linear graft (C_3F_7; Figure 2 and Table 2). The hysteresis also showed to be increased compared to the linear graft. The graft-on-graft architecture functionalized with $C_{15}H_{31}$ exhibited a CA of 165°, which is an improvement compared to the linear brush ($C_{15}H_{31}$; Figure 2 and Table 2). The hysteresis for this alkyl-functionalized surface was comparable to that of the C_7F_{15} surface (5°). The wettability of the graft-on-graft architecture functionalized with PDMS was reduced (CA 162°) compared to that of the single graft (PDMS; Figure 2 and Table 2). The hysteresis for the PDMS-functionalized graft-on-graft surface reached a level similar to that observed for the single graft surface.

Long-Term Hydrophobic Properties. CA measurements over time showed an improvement for all surfaces when compared to the linear graft modification. For the C_7F_{15}-functionalized surface, the CA only decreased slightly over time (from 172° to 164°), and the surface was still superhydrophobic after 1 h (Figure 3).

In addition, the surface postfunctionalized with C_3F_7 was observed to be superhydrophobic after 1 h, with the CA decreasing from 162° to 156°, showing that the graft-on-graft architecture also provides improved long-time stability in this case in accordance with the observation for the C_7F_{15}-modified graft-on-graft surface. The $C_{15}H_{31}$-functionalized

Scheme 2. Synthetic Approach to Graft-on-Graft Functionalization of Bio-Fiber Surfaces[a]

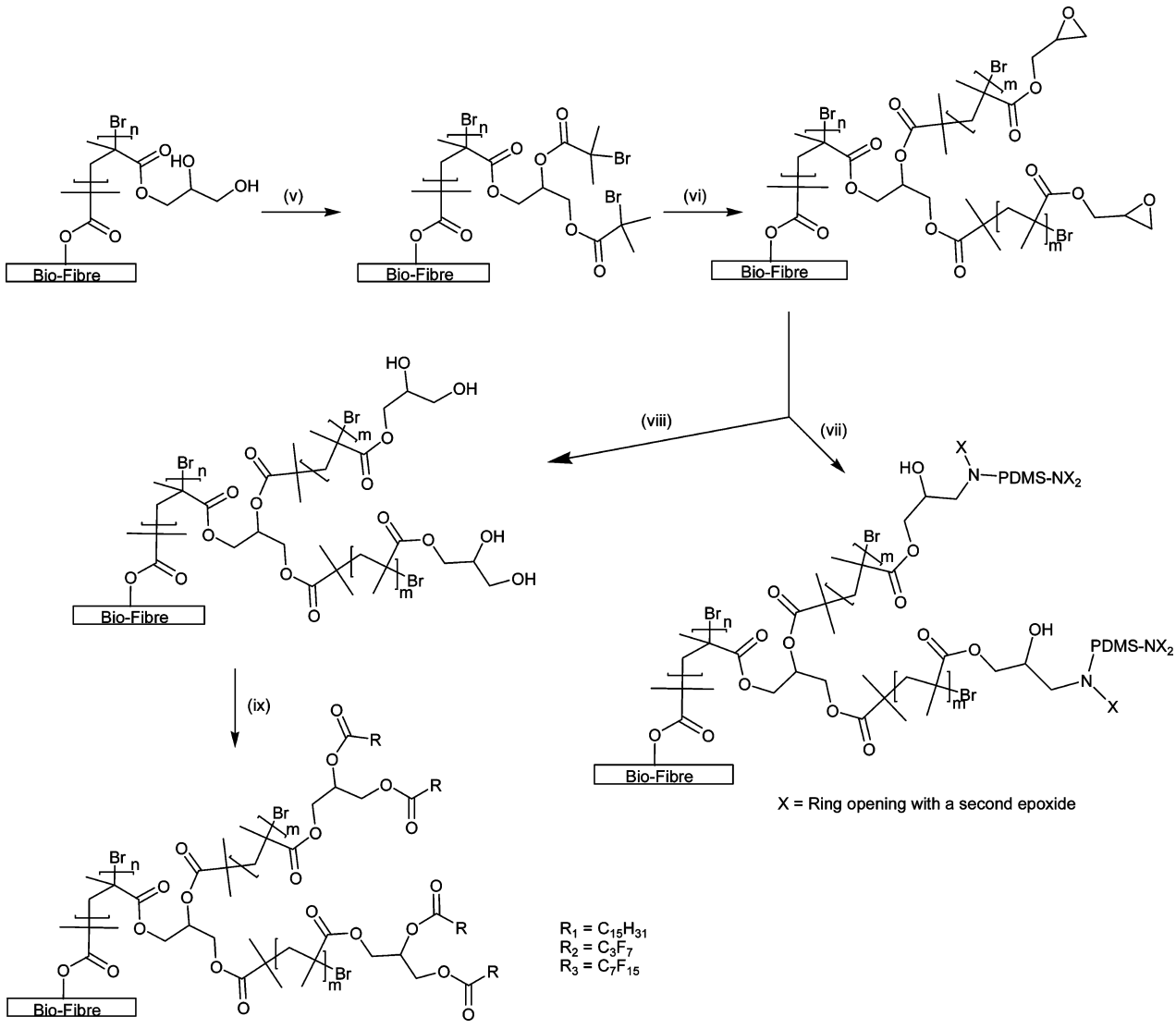

[a] Conditions: (v) 2-bromoisobutyryl bromide, TEA, DMAP, DCM, RT; (vi) GMA, $Cu^{I}Cl$, $Cu^{II}Br_2$, PMDETA, toluene, 30 °C; (vii) toluene, bis(3-aminopropyl)-terminated PDMS, 100 °C; (viii) HCl(aq), THF, RT; (ix) acid chloride (R1−R3), TEA, DMAP, DCM, RT.

Table 2. CA Results Obtained for PGMA Graft-on-Graft Architectures Modified with Different Low-Energy Compounds

	CA (deg)			
graft-on-graft	static	advancing	receding	hysteresis
PGMA-*g*-PGMA−C_7F_{15}	172	173	168	5
PGMA-*g*-PGMA−C_3F_7	162	164	156	9
PGMA-*g*-PGMA−$C_{15}H_{31}$	165	167	162	5
PGMA-*g*-PGMA−PDMS	162	164	154	10

surface also showed a significantly more stable CA over time, compared to that of the linear graft. The CA decreased from 165 to 147° over 1 h, which is a larger decrease compared to the fluorinated surfaces, but interestingly still showing a virtually retained superhydrophobicity (Figure 3).

The PDMS-functionalized surface showed a decrease in the CA over 1 h from 162 to 143°. The hydrophobicity of this surface is overall more comparable to that of the linear graft functionalized with C_7F_{15}.

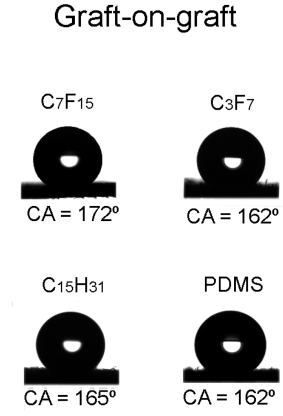

FIGURE 2. CA images for PGMA graft-on-graft architectures modified with different low-energy compounds (Table 2).

Oleophobicity. To investigate the oil repellence (oleophobic properties) of the modified cellulose surface, a drop of sunflower oil was added on the surface, and the CA was

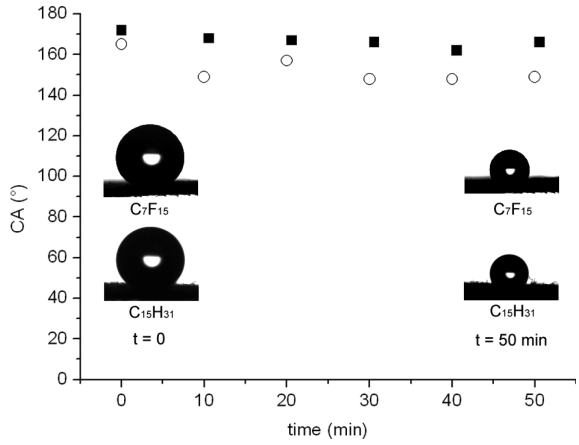

FIGURE 3. Water CAs measured over time for PGMA-*g*-PGMA filter paper functionalized with C_7F_{15} (■) and $C_{15}H_{31}$ (○), respectively. The size of the droplets decreases with time because of evaporation.

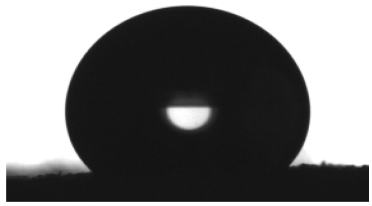

FIGURE 4. CA image of an oil droplet applied to the C_7F_{15}-functionalized graft-on-graft surface.

measured. For the C_7F_{15}-modified surface, the static oil CA was 144°, meaning that the surface is highly oleophobic (Figure 4).

The C_3F_7-modified graft-on-graft surface was found to possess lower oleophobic properties (oil CA 124°) as compared to the C_7F_{15}-modified graft-on-graft surface. The alkyl- and PDMS-modified surfaces were not oleophobic, and the oil drop was adsorbed into these surfaces as expected.

Surface Structure. Because the surface structure is important for the superhydrophobic properties of a material, the postfunctionalized graft-on-graft-modified surfaces were also characterized using tapping-mode AFM. As reported previously, for the C_7F_{15}-modified graft-on-graft bio-fiber surface, AFM imaging showed that the grafted polymer almost completely covered the fibrils and, in addition, nanosized features were observed, displaying a micro-nano-binary structure (29). AFM analysis of the C_3F_7-functionalized surface showed a surface structure similar to that of the C_7F_{15}-functionalized surface with fewer nanosized features.

The $C_{15}H_{31}$-functionalized graft-on-graft surfaces showed superhydrophobicity similar to that of the C_7F_{15}-modified

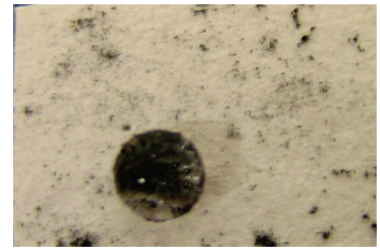

FIGURE 6. Self-cleaning ability of a $C_{15}H_{31}$-modified graft-on-graft surface.

surface, and interestingly AFM analysis showed that the surface structure of these two surfaces also seems to be very similar (Figure 5a) in the sense that the fibrils are almost completely covered and both micro- and nanosized features can be observed. The nanosized features on the $C_{15}H_{31}$-modified surface were even more prominent in the AFM phase image compared to those of the C_7F_{15}-modified surface, which might be due to the difference in moduli between the polymers in the graft-on-graft structure and the attached $C_{15}H_{31}$ (Figure 5b). When one of these structures is magnified and the height profile is extracted from the height image, the actual height of the feature can be estimated and is measured to approximately 50 nm (Figure 5c,d).

AFM analysis of the PDMS-functionalized surface revealed a significantly smoother surface topography as compared to that of the C_7F_{15}-modified graft-on-graft surface. The surface appears to be covered by the grafted polymer, and only microsized features can be observed because the nanosized features are absent (see the Supporting Information).

Self-Cleaning Properties. For a surface to be self-cleaning, a low hysteresis in the CA is necessary. The lowest hysteresis was observed for the C_7F_{15}- and $C_{15}H_{31}$-functionalized graft-on-graft samples, and as expected, these two surfaces did show self-cleaning properties. We earlier demonstrated that a C_7F_{15}-functionalized graft-on-graft cellulose surface is self-cleaning; carbon black powder applied to the surface can easily be removed when a water droplet is allowed to roll over the surface (29).

The self-cleaning properties of the $C_{15}H_{31}$-functionalized graft-on-graft surface could also be demonstrated by applying carbon black powder to the surface. The water droplet adsorbed the carbon black powder as it rolled over the surface, and it is clearly seen that the droplet is covered with the powder (Figure 6).

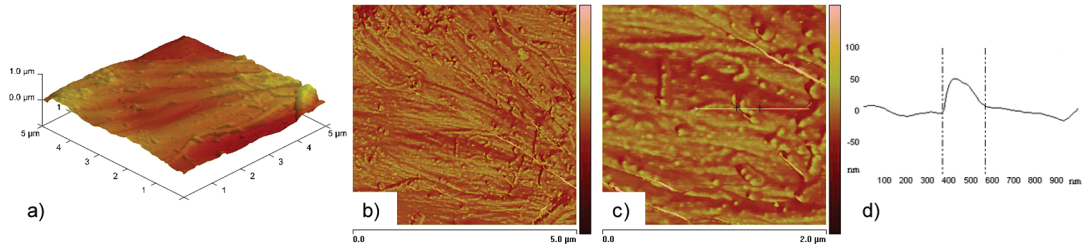

FIGURE 5. (a) Tapping-mode AFM surface plot of filter paper with a graft-on-graft architecture and postfunctionalization with $C_{15}H_{31}$. (b and c) Tapping-mode AFM phase images of $C_{15}H_{31}$-functionalized graft-on-graft surfaces: (b) 5 × 5 μm image; (c) enlargement of the image of 2 × 2 μm. (d) Height profile extracted from the corresponding height image (the scale on the *y* axis is ±100 nm).

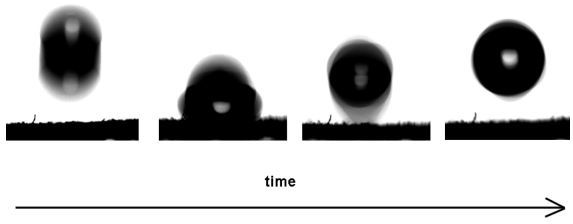

FIGURE 7. Water droplet bouncing on the $C_{15}H_{31}$-modified graft-on-graft surface (approximately 10 ms between each picture).

To further verify the superhydrophobic nature of the $C_{15}H_{31}$-modified graft-on-graft surface, a water droplet was allowed to fall onto the surface. It was observed that the droplet bounced back up after impact with the surface, meaning that the droplet acts like a spring and recovers its spherical shape rapidly (Figure 7), similar to the findings reported by Callies and Quéré (20). If the bio-fiber surface was tilted before the water droplet hit the surface, the droplet bounced off. This is of great importance in applications such as water-repellent clothing, in order to avoid wetting of the surface.

CONCLUSION

This work has demonstrated versatile routes for the fabrication of superhydrophobic biofiber surfaces using low amounts or complete removal of fluorinated compounds. The surfaces possessing the highest hydrophobicity (static CA and CA stability over time) were obtained via a graft-on-graft architecture based on PGMA brushes. The epoxide groups in the graft-on-graft architecture were subsequently used for the attachment of hydrophobic compounds directly or after being hydrolyzed under acidic conditions. The formed hydroxyl groups are available for acylation reactions in order to incorporate low surface energy acid chlorides. The obtained surfaces showed low hysteresis and extremely high water CAs, reaching a maximum of 172° for the C_7F_{15}-modified graft-on-graft architecture. The fluorinated graft-on-graft surfaces were also found to be oleophobic because a droplet of sunflower oil applied to these surfaces exhibited CAs ranging between 124 and 144°.

Superhydrophobic (CA 165°) and self-cleaning surfaces with good long-term stability could be obtained without the use of any fluorine-containing compounds when sufficiently long alkyl chains ($C_{15}H_{31}$) were attached to the modified graft-on-graft bio-fiber surface. Also, a water droplet allowed to fall onto the surface bounced back up after impact and recovered its spherical shape. AFM analysis showed that this surface possessed a micro/nanobinary surface structure, similar to what was observed for the C_7F_{15}-modified surface. These results show that it is possible to obtain superhydrophobic surfaces even via nonfluorinating postfunctionalization of branched PGMA grafts.

We believe that our findings regarding the ability to fabricate superhydrophobic and self-cleaning surfaces using more environmentally friendly and less expensive compounds, such as long alkyl chains, will prove to be extremely useful in the field of surface modification.

Acknowledgment. We acknowledge BiMaC (Biofibre Materials Centre), BioMime (Swedish Center for Biomimetic Fiber Engineering), The Swedish Research Council, Wilhelm Beckers Jubileumsfond, and The Research Council of Norway within the NanoMat program, project "Dendritic nanoporous materials with multifunctionality" (no. 163529/S10), for financial support. Niklas Nordgren is acknowledged for assistance with AFM analysis.

Supporting Information Available: FT-IR spectra and additional AFM images. This material is available free of charge via the Internet at http://pubs.acs.org.

REFERENCES AND NOTES

(1) Nakajima, A.; Hashimoto, K.; Watanabe, T. *Monatsh. Chem.* **2001**, *132*, 31.
(2) Zhang, X.; Shi, F.; Niu, J.; Jiang, Y.; Wang, Z. *J. Mater. Chem.* **2008**, *18*, 621–633.
(3) Barthlott, W.; Neinhuis, C. *Planta* **1997**, *202*, 1–8.
(4) Gao, X.; Jiang, L. *Nature* **2004**, *432*, 36.
(5) Xie, Q.; Fan, G.; Zhao, N.; Guo, X.; Xu, J.; Dong, J.; Zhang, L.; Zhang, Y.; Han, C. C. *Adv. Mater.* **2004**, *16*, 1830–1833.
(6) Zhao, N.; Xu, J.; Xie, Q.; Weng, L.; Guo, X.; Zhang, X.; Shi, L. *Macromol. Rapid Commun.* **2005**, *26*, 1075–1080.
(7) Guo, Z.; Zhou, F.; Hao, J.; Liu, W. *J. Am. Chem. Soc.* **2005**, *127*, 15670–15671.
(8) Yamanaka, M.; Sada, K.; Miyata, M.; Hanabusa, K.; Nakano, K. *Chem. Commun.* **2006**, 2248–2250.
(9) Roig, A.; Molins, E.; Rodríguez, E.; Martínez, S.; Moreno-Mañas, M.; Vallribera, A. *Chem. Commun.* **2004**, 2316–2317.
(10) Shirtcliffe, N. J.; McHale, G.; Newton, M. I.; Perry, C. C.; Roach, P. *Chem. Commun.* **2005**, 3135–3137.
(11) Yabu, H.; Takebayashi, M.; Tanaka, M.; Shimomura, M. *Langmuir* **2005**, *21*, 3235–3237.
(12) Ma, M.; Mao, Y.; Gupta, M.; Gleason, K. K.; Rutledge, G. C. *Macromolecules* **2005**, *38*, 9742–9748.
(13) Zhang, G.; Wang, D.; Gu, Z.-Z.; Möhwald, H. *Langmuir* **2005**, *221*, 9143–9148.
(14) Li, S.; Li, H.; Wang, X.; Song, Y.; Liu, Y.; Jiang, L.; Zhu, D. *J. Phys. Chem. B* **2003**, *106*, 9274–9276.
(15) Gu, Z.-Z.; Uetsuka, H.; Takahashi, K.; Nakajima, R.; Onishi, H.; Fujishima, A.; Sato, O. *Angew. Chem., Int. Ed.* **2003**, *42*, 894–897.
(16) Roach, P.; Shirtcliffe, N. J.; Newton, M. I. *Soft Matter* **2008**, *4*, 224–240.
(17) Chen, W.; Fadeev, A. Y.; Hsieh, M. C.; Öner, D.; Youngblood, J.; McCarthy, T. J. *Langmuir* **1999**, *15*, 3395–3399.
(18) Öner, D.; McCarthy, T. J. *Langmuir* **2000**, *16*, 7777–7782.
(19) Youngblood, J. P.; McCarthy, T. J. *Macromolecules* **1999**, *32*, 6800–6806.
(20) Callies, M.; Quéré, D. *Soft Matter* **2005**, *1*, 55–61.
(21) Lafuma, A.; Quéré, D. *Nat. Mater.* **2003**, *2*, 457–460.
(22) Blossey, R. *Nat. Mater.* **2003**, *2*, 301–306.
(23) Cassie, A.; Baxter, S. *Trans. Faraday Soc.* **1944**, 546–451.
(24) Hebeish, A.; Guthrie, J. T. *Polymers: The Chemistry and Technology of Cellulosic Copolymers*; Springer-Verlag: Berlin, 1981; Vol. 4, p 351.
(25) Vigo, T. L. *Polym. Adv. Technol.* **1998**, *9*, 539–548.
(26) Carlmark, A.; Malmström, E. *J. Am. Chem. Soc.* **2002**, *124*, 900–901.
(27) Carlmark, A.; Malmström, E. E. *Biomacromolecules* **2003**, *4*, 1740–1745.
(28) Lindqvist, J.; Malmström, E. *J. Appl. Polym. Sci.* **2006**, *100*, 4155–4162.
(29) Nyström, D.; Lindqvist, J.; Östmark, E.; Hult, A.; Malmström, E. *Chem. Commun.* **2006**, 3594–3596.
(30) Östmark, E.; Harrison, S.; Wooley, K. L.; Malmström, E. E. *Biomacromolecules* **2007**, *8*, 1138–1148.
(31) Östmark, E.; Nyström, D.; Malmström, E. *Macromolecules* **2008**, *41*, 4405–4415.
(32) Lindqvist, J.; Nyström, D.; Östmark, E.; Antoni, P.; Carlmark, A.; Johansson, M.; Hult, A.; Malmström, E. *Biomacromolecules* **2008**, *9*, 2139–2145.
(33) Westlund, R.; Carlmark, A.; Hult, A.; Malmström, E.; Saez, I. M. *Soft Matter* **2007**, *3*, 866–871.
(34) Wang, J.-S.; Matyjaszewski, K. *Macromolecules* **1995**, *28*, 7901–7910.

(35) Wang, J.-S.; Matyjaszewski, K. *J. Am. Chem. Soc.* **1995**, *117*, 5614–5615.
(36) Kato, M.; Kamigaito, M.; Sawamoto, M.; Higashimura, T. *Macromolecules* **1995**, *28*, 1721–1723.
(37) Yin, M.; Habicher, W. D.; Voit, B. *Polymer* **2005**, *46*, 3215–3222.
(38) Pilon, L. N.; Armes, S. P.; Findlay, P.; Rannard, S. P. *Eur. Polym. J.* **2006**, *42*, 1487–1498.
(39) Shah, R. R.; Merreceyes, D.; Husemann, M.; Rees, I.; Abbott, N. L.; Hawker, C. J.; Hedrick, J. L. *Macromolecules* **2000**, *33*, 597–605.
(40) Kim, J.-B.; Bruening, M. L.; Baker, G. L. *J. Am. Chem. Soc.* **2000**, *122*, 7616–7617.
(41) Von Werne, T.; Patten, T. E. *J. Am. Chem. Soc.* **1999**, *121*, 7409–7410.
(42) Zhao, B.; Brittain, W. J. *J. Am. Chem. Soc.* **1999**, *121*, 3557–3558.
(43) Husseman, M.; Malmström, E. E.; McNamara, M.; Mate, M.; Mecerreyes, D.; Benoit, D. G.; Hedrick, J. L.; Mansky, P.; Huang, E.; Russell, T. P.; Hawker, C. J. *Macromolecules* **1999**, *32*, 1424–1431.
(44) Ejaz, M.; Yamamoto, S.; Ohno, K.; Tsujii, Y.; Fukuda, T. *Macromolecules* **1998**, *31*, 5934–5936.
(45) Liu, T.; Casado-Portilla, R.; Belmont, J.; Matyjaszewski, K. *J. Polym. Sci., Part A: Polym. Chem.* **2005**, *43*, 4695–4709.
(46) Kong, H.; Gao, C.; Yan, D. *J. Am. Chem. Soc.* **2004**, *126*, 412–413.
(47) Plackett, D.; Jankova, K.; Egsgaard, H.; Hvilsted, S. *Biomacromolecules* **2005**, *6*, 2474–2484.
(48) Ramakrishnan, A.; Dhamodharan, R.; Rühe, J. *J. Polym. Sci., Part A: Polym. Chem.* **2006**, *44*, 1758–1769.
(49) Wang, T.; Hu, X.; Dong, S. *Chem. Commun.* **2007**, 1849–1851.
(50) Hoefnagels, H. F.; Wu, D.; de With, G.; Ming, W. *Langmuir* **2007**, *23*, 13158–13163.
(51) Ramaratnam, K.; Tsyalkovsky, V.; Klep, V.; Luzinov, I. *Chem. Commun.* **2007**, 4510–4512.
(52) Gao, L.; McCarthy, T. J. *Langmuir* **2006**, *22*, 5998–6000.
(53) Balu, B.; Breedveld, V.; Hess, D. W. *Langmuir* **2008**, *24*, 4785–4790.
(54) Li, S.; Zhang, S.; Wang, X. *Langmuir* **2008**, *24*, 5585–5590.
(55) Xu, F. J.; Zhong, S. P.; Yung, L. Y. L.; Tong, Y. W.; Kang, E.-T.; Neoh, K. G. *Biomaterials* **2006**, *27*, 1236–1245.
(56) Edmondson, S.; Huck, W. T. S. *J. Mater. Chem.* **2004**, *14*, 730–734.
(57) Edmondson, S.; Huck, W. T. S. *Adv. Mater.* **2004**, *16*, 1327–1331.
(58) Tsarevsky, N. V.; Bencherif, S. A.; Matyjaszewski, K. *Macromolecules* **2007**, *40*, 4439–4445.
(59) Cummins, D.; Wyman, P.; Duxbury, C. J.; Thies, J.; Koning, C. E.; Heise, A. *Chem. Mater.* **2007**, *19*, 5285–5292.

AM800235E